

Far-infrared picosecond time-resolved measurement of the free-induction decay in GaAs:Si

P. C. M. Planken,* P. C. van Son, J. N. Hovenier, T. O. Klaassen, and W. Th. Wenckebach
Department of Applied Physics, Delft University of Technology, P.O. Box 5046, 2600 GA Delft, The Netherlands

B. N. Murdin and G. M. H. Knippels
FOM-Institute for Plasma Physics "Rijnhuizen," 3430 BE Nieuwegein, The Netherlands
 (Received 26 July 1994; revised manuscript received 5 December 1994)

By measuring changes in the photoconductivity induced by picosecond far-infrared pulse pairs from a free-electron laser, we have time resolved the free-induction decay of the $1s-210$ and $1s-2p^+$ Si-shallow-donor transitions in bulk GaAs. The method frees us from the problem of measuring the optical emission of the transitions and allows us to obtain their dephasing times. We expect to be able to use the same method in the future to measure other coherent phenomena in these systems, such as photon echoes.

I. INTRODUCTION

In optical experiments in gases, liquids, and solids, ultrashort visible or near-IR laser pulses are commonly used to probe the dynamics of the system under study. Examples are free-induction decay measurements to obtain optical dephasing times of transitions, pump-probe techniques to measure excited-state lifetimes, and four-wave mixing to measure phonon echoes.^{1,2} When transitions have frequencies in the far-infrared region, it is sometimes possible to probe their dynamics with ultrashort visible pulses using nonlinear techniques such as Raman scattering.² In many cases, however, the use of visible pulses also creates many undesirable simultaneous excitations such as the creation of electron-hole pairs by interband excitation. Worse, the high-intensity visible pulses usually needed for these nonlinear time-resolved experiments may cause irreversible damage to the material under study. As a result, direct excitation with far-infrared lasers is needed. However, time-resolved studies of the dynamics of these transitions with ultrashort pulses were hampered by the absence of suitable ultrashort-pulse far-infrared laser sources.³

In this paper, we use picosecond, far-infrared pulses from the free-electron laser for infrared experiments (FELIX) at the FOM Institute Rijnhuizen, to time resolve the free-induction decay of the $1s-2p^+$ and the $1s-210$ silicon (Si) shallow-donor transitions in GaAs. We avoid the problem of detecting the emitted far-infrared radiation by using a detection method based on the photoconductive response⁴⁻⁶ of the sample. Two pulses, separated in time, excite the system. We find that the second, delayed pulse induces changes in the photoconductivity of the sample that depend on the optical phase difference between the two pulses. We prove that these phase-difference-dependent changes reflect changes in the excited-state population of the Si donors, caused by the coherent manipulation by the second pulse of the optical polarization stored in the donor system by the first. By measuring how these coherent population changes decrease in magnitude for increasing pulse separations, we

can obtain the picosecond free-induction decay time constant of the optical polarization of the Si donor. Thus, instead of a (difficult) time-resolved measurement of the far-infrared optical emission of the free-induction decay, we do a time-resolved measurement of the decay of the coherence that is the source of the emission. We expect that this method can also be used to measure various other coherent phenomena such as photon echoes.

II. EXPERIMENT

Our sample, obtained from Philips Research Laboratory, Redhill, U.K., is a $10\text{-}\mu\text{m}$ -thick Si-doped GaAs layer grown on a $400\text{-}\mu\text{m}$ -thick semi-insulating GaAs crystal. The doping density N_d is approximately $5 \times 10^{14} \text{ cm}^{-3}$, and $N_a \leq 1 \times 10^{14} \text{ cm}^{-3}$. Sn contacts have been diffused in for conductivity measurements. The experiments are done at 8 K in a magnet cryostat in magnetic fields up to 9 T. The magnetic field can be adjusted to tune the various donor transitions into resonance with a particular far-infrared frequency.

Tunable far-infrared pulses are generated by the FELIX. The light emerges from the FELIX in the form of pulse trains consisting of approximately 5000 micropulses. The pulse trains are generated at a 5-Hz repetition rate. The micropulses have an adjustable duration of a few picoseconds and are separated by a nanosecond. After passing through an attenuator, used to avoid saturation of the transitions, they are sent into a Michelson interferometer which contains a $6\text{-}\mu\text{m}$ -thick Mylar beamsplitter. One arm of the Michelson can be scanned with respect to the other so that the pulse pairs emerging from the Michelson have an adjustable time separation. The pulse pairs are focused onto the sample with a 50-cm focal-length polyethylene lens, and the radiation enters the cryostat through two polyethylene windows. Care is taken not to illuminate the contacts on the sample to avoid spurious signals. The magnetic field is perpendicular to the surface of the sample and perpendicular to the polarization of the laser pulses. The whole setup is enclosed in a box that is continuously flushed with dry ni-

trogen gas to reduce water vapor absorption. The high-ohmic sample is voltage biased. The current response of the sample is measured with a time resolution of $0.1 \mu\text{s}$, and follows the amplitude envelope of the FELIX pulse train.

III. RESULTS

A. Si-donor optical spectrum

To identify the Si-donor transitions in the sample,⁵ we measure the photoconductivity as a function of magnetic field for an excitation frequency of 4.45 THz (Fig. 1). The magnetic field shifts the transition frequencies, and for fields larger than a few T the shift is linearly proportional to the field. For this measurement, the pulse duration was lengthened to $> 10 \text{ ps}$ to decrease the frequency bandwidth of the pulse while one arm of the Michelson was blocked. Figure 1 shows peaks in the photoconductivity whenever a Si-donor transition is resonant with the excitation pulse. The transitions are visible in photoconductivity measurements because most electrons in the excited states decay to the conduction band of the GaAs crystal, where we can use conventional, relatively slow electronics to detect them.⁵ The photoconductivity change is linearly proportional to the excited-state population. The electrons return to the $1s$ ground state of the donor atom after roughly 100 ns . To avoid significant depopulation of the ground state by the cumulative effect of hundreds of micropulses, we keep the micropulse energy in the following experiments lower than 10 nJ . In the figure the $1s-2p^+$ and $1s-210$ transitions are marked. They are the two strongest transitions on which we will focus our attention.

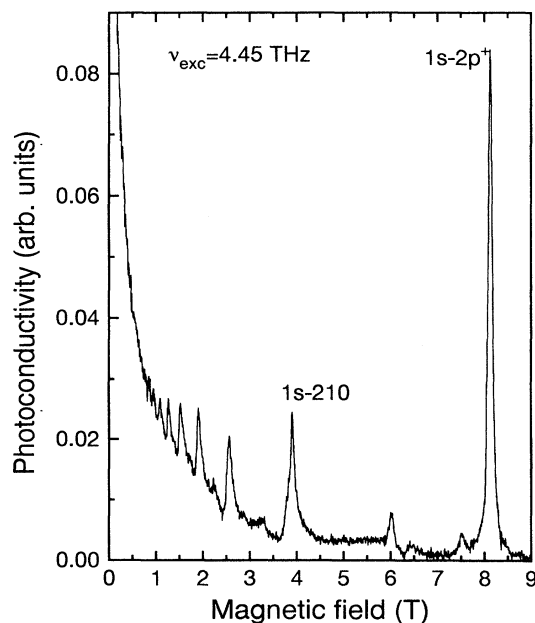


FIG. 1. Measured photoconductivity vs magnetic field for an excitation frequency of 4.45 THz . In the spectrum, the $1s-2p^+$ and the $1s-210$ transitions discussed in the text are marked.

B. Time-resolved measurements: resonant case

In Fig. 2(a) we plot the photoconductivity of the sample as a function of the time separation between the two pulses from the Michelson at an excitation frequency of 4.38 THz (corresponding to a wavelength of $68.8 \mu\text{m}$) and $B = 0 \text{ T}$. The photoconductivity oscillates when the time separation between the two pulses increases, and the oscillation period is given by the excitation wavelength. At this magnetic-field strength, the far-infrared photons directly excite electrons from the $1s$ ground state of the Si donor to a broad continuum of conduction-band states.⁵ As a result, the sample acts as broadband frequency-independent detector. The oscillations are explained by the temporal overlap of the two pulses on the beamsplitter of the Michelson, and Fig. 2(a) therefore represents the field autocorrelation of the exciting pulses. From the autocorrelation we deduce a pulse duration of approximately 3 ps , assuming bandwidth-limited pulses.⁷

When the laser is resonant with the $1s-2p^+$ transition, the results are markedly different [Fig. 2(b)]. In contrast to the results in Fig. 2(a), the oscillations in the photoconductivity (seen more clearly in the inset) are still present for large time separations when the two pulses have no temporal overlap on the beamsplitter. The oscillations eventually decrease in amplitude and, after 50 ps , they can no longer reliably be measured. In Fig. 2(c) we plot the photoconductivity of the sample versus time separation when the laser is resonant with the $1s-210$ transition. Here the measured oscillation amplitude decays much more quickly for increasing time separation, although

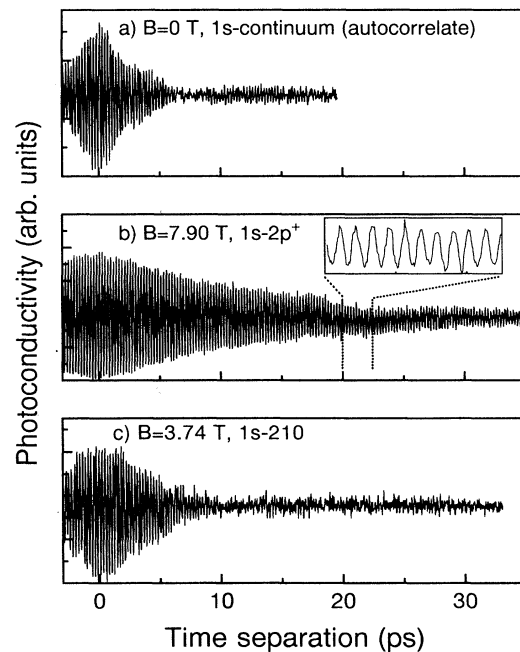


FIG. 2. Measured photoconductivity as a function of pulse separation for three different transitions: $1s$ continuum (a), $1s-2p^+$ (b), and the $1s-210$ (c). The excitation frequency was 4.38 THz . The inset in (b) shows a small section of the curve, magnified a few times.

significantly more slowly compared to the autocorrelation of the pulses in Fig. 2(a). Clearly, the above results provide evidence that the medium only has a memory for the phase of the exciting electric field when the laser is resonant with a (discrete) transition in the donor system. For pulse energies lower than 10 nJ, we observe no dependence of the decay times on the energy of the micropulses. Above 10 nJ possible energy-dependent effects are obscured by the cumulative depopulation of the ground state by hundreds of micropulses.

C. Time-resolved measurements: nonresonant case

If we detune the transitions with respect to the central wavelength of the pulses, by changing the magnetic field slightly, the results change dramatically. In Fig. 3 we show measurements of the photoconductivity for excitation of the $1s-2p^+$ transition for three different values of the detuning. When the laser is exactly resonant with the transition, we obtain the curve already shown in Fig. 2(b) and reproduced in Fig. 3(a). When we now detune the transition 0.08 ± 0.01 THz away from the central wavelength of the laser, we obtain the result in Fig. 3(b). In addition to a decrease in the absolute value (not shown here) of the photoconductivity compared to Fig. 3(a), the signal also has a different shape. After an apparent fast decay of the oscillation amplitude for pulse separations up to 5 ps, a slower decay is seen for larger values of the pulse separation. When we increase the detuning to a value of 0.13 ± 0.01 THz we measure the curve shown in Fig. 3(c). Again the photoconductivity is smaller than in

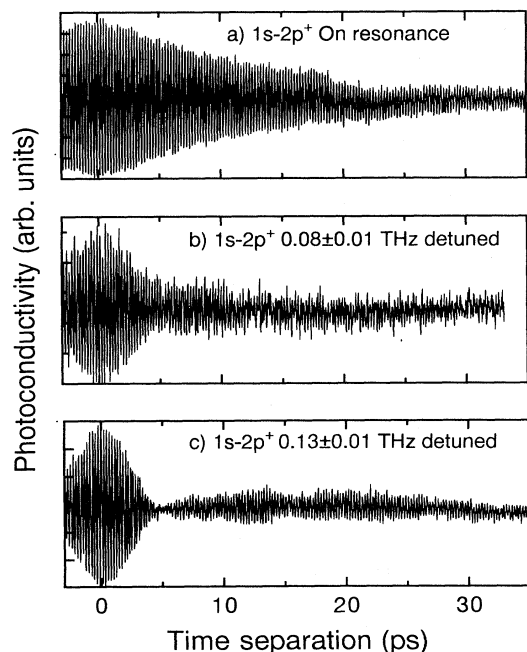


FIG. 3. Measured photoconductivity as a function of pulse separation when the laser excites the $1s-2p^+$ transition, for three different values of the detuning. Detuning is accomplished by detuning the transition while keeping the excitation frequency constant.

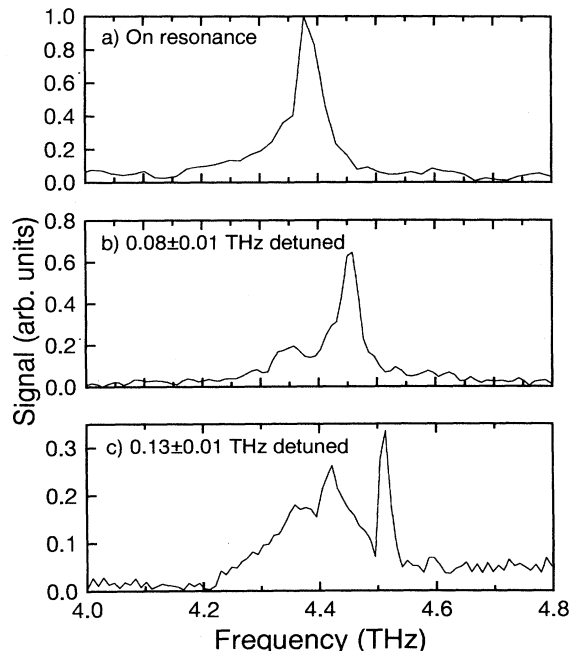


FIG. 4. Calculated Fourier transforms of the measured curves in Fig. 3. The sharp feature corresponds to the $1s-2p^+$ transition. The broad background represents the autocorrelation of the laser pulses. The excitation frequency was 4.38 THz. The three Fourier transforms have the same arbitrary units on the vertical axis.

Fig. 3(b) and the initial fast decay of the oscillation amplitude is followed by what seems to be a revival, with a node at $t \approx 4$ ps. Both in Figs. 3(b) and 3(c), oscillations are still observed for pulse separations of several tens of picoseconds as in Fig. 3(a), with the difference that they are reduced in amplitude.

The oscillations in the photoconductivity shown in Fig. 3 have two contributions. This is clearly demonstrated in Fig. 4, where we plot the Fourier transforms of the signals. A broad peak represents the power spectrum of the laser pulses. Superimposed on this is a much narrower feature that shifts in frequency when the $1s-2p^+$ transition is detuned from the central wavelength of the pulses. It corresponds to the oscillations that are visible in Fig. 3 for time separations larger than 5 ps, when the pulses have no temporal overlap. This observation proves that the oscillations in the photoconductivity for pulse separations larger than the pulse duration are indeed caused by a memory effect in the Si-donor transitions.

IV. THEORY

To explain our results, we use a two-level system to model the Si-donor transitions. The oscillations in the photoconductivity as a function of the time separation between the two pulses represent oscillations in the population of the excited states of the Si donor⁵ due to the combined effect of the two pulses. When τ is larger than the pulse duration, they are explained by the interference

of the electric field of the second pulse with the coherence or optical polarization, stored in the medium by the first pulse. For the complex electric-field amplitude of the exciting pulse pair, we have

$$E_0(t) = A_0(t) + A_0(t - \tau)e^{-i\omega_L\tau}. \quad (1)$$

Using a density-matrix formulation we can write the following well-known coupled differential equations for the ground-state population ρ_{11} , the excited-state population ρ_{22} , and the slowly varying coherence amplitude ρ_{12} :⁸

$$\begin{aligned} \frac{\partial \rho_{22}}{\partial t} &= -\frac{\rho_{22}}{T_{22}} - \frac{i}{\hbar}(\mu_{12}E_0^* \rho_{21} - \mu_{21}E_0 \rho_{12}), \\ \frac{\partial \rho_{11}}{\partial t} &= -\frac{\partial \rho_{22}}{\partial t}, \\ \frac{\partial \rho_{12}}{\partial t} &= i\rho_{12}(\omega_L - \omega_{12}) - \frac{\rho_{12}}{T_{12}} + \frac{i}{\hbar}\mu_{12}E_0^*(\rho_{22} - \rho_{11}). \end{aligned} \quad (2)$$

Here $A_0(t)$ is the Gaussian envelope of the pulses, τ is their time separation, ω_L is the central frequency of the laser, μ_{12} is the transition-dipole moment, ω_{12} is the transition frequency, T_{22} is the excited-state lifetime, and T_{12} is the optical dephasing time. To obtain (2), the rotating-wave approximation was used.

We simulate the experiment by numerically integrating (2) for a large number of values of the optical pulse separation τ . Figure 5 is a plot of the calculated final excited-state population ρ_{22} as a function of τ , for the three different values of the detuning shown in Fig. 4. The calculations are in good qualitative agreement with

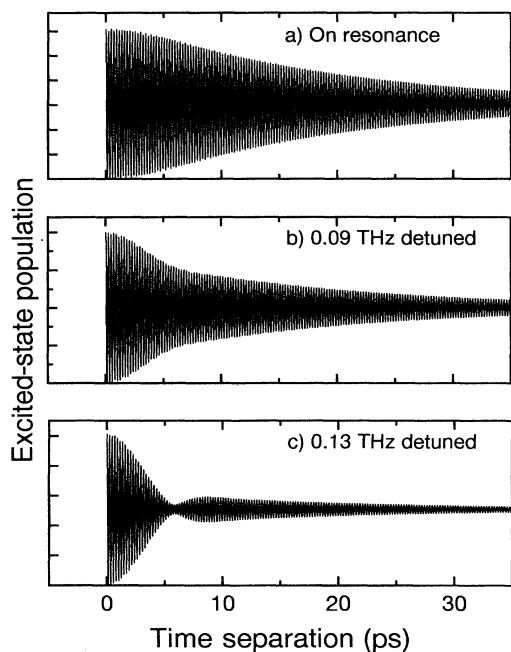


FIG. 5. Calculated excited-state population vs time separation for three different values of the detuning. We assume Gaussian pulses of 3.75-ps duration and a value of $T_{12} = 18$ ps. The population lifetime is assumed to be infinite.

the experimental results for a value of T_{12} of approximately 18 ps. The pulse duration was assumed to be 3.75 ps, and $T_{22} \gg T_{12}$. Similar calculations for the 1s-210 transition give us an approximate value of $T_{12} = 5$ ps (not shown here).

V. DISCUSSION

The good agreement between the calculations and the experimental results, and a closer inspection of Eq. (2), lead to the following picture of the excitation and measurement processes. The first pulse induces a coherent time-dependent optical polarization (memory) $P(t) = 2N \text{Re}(\rho_{12}(t)\mu_{12})$, and transfers population into the excited state of the two-level system. After the first pulse, the optical polarization $P(t)$ decays with time constant T_{12} due to dephasing processes. If the second pulse arrives before dephasing is complete, the electric field of the second pulse can coherently interfere with the optical polarization. This will lead to enhanced excitation to, or deexcitation of, the upper state depending on the phase difference between the electric field of the second pulse and the optical polarization. The final excited-state population therefore oscillates when the phase difference is varied, which is accomplished by varying the pulse separation.^{9,10} If the dephasing of the optical polarization is complete before the second pulse arrives, the excited-state population does not depend on the optical phase difference. Hence, by measuring the coherent population changes as a function of τ , we obtain the decay time constant T_{12} of the optical polarization. Note that in our experiment we can monitor the excited-state population by measuring the photoconductivity of the sample.

The apparent faster dephasing time of the 1s-210 that we find is consistent with the character of the 210 state as an autoionizing state with a lifetime much shorter than the $2p^+$ state.^{5,11} We would like to point out that the assumption $T_{12} \ll T_{22}$, used in the numerical integration of (2), is a realistic one for the 1s- $2p^+$ transition, justified by frequency-domain measurements on samples with a lower donor concentration. There it was found that the $2p^+$ excited-state population lifetime is at least several hundred ps.¹² The lifetime T_{22} of the 210 state, however, is probably short^{5,11} enough that we need its value in the future for an accurate determination of the dephasing time of the 1s-210 transition.

When the 1s- $2p^+$ transition is detuned with respect to the central frequency ω_L of the laser, the induced optical polarization oscillates at the transition frequency ω_{12} , which is different from the central laser frequency. The second pulse interferes both with the electric field of the first pulse on the beamsplitter (for small τ), and the induced optical polarization in the sample. The Fourier transforms of the photoconductivity measurements will therefore show two peaks (Fig. 4): a broad one that corresponds to ω_L and a narrow one that corresponds to ω_{12} . We can also understand our time-domain measurements using time-domain arguments. For example, for a certain τ the electric field of the second pulse can be in phase with the electric field of the first pulse and simultaneously out of phase with the induced polarization. When we

now change the pulse separation by approximately π/ω_{12} the situation is reversed: the electric field of the second pulse is out of phase with the electric field of the first pulse, but in phase with the induced polarization. Both effects compensate each other, giving a zero net change of the excited-state population. For pulse separations in between, both effects also cancel each other. Consequently, a plot of the excited state population versus pulse separation will show a node as in Fig. 3(c).

Note that the parameters used in the calculations were chosen for maximum qualitative agreement between the calculations and the experimental results, and are slightly different from those in the experiments. For instance, we assume that the excitation pulses have a Gaussian temporal envelope of 3.75-ps duration. In contrast, from the autocorrelation measurement in Fig. 2(a), we can see that the pulses used in the experiment clearly have a non-Gaussian temporal envelope of roughly 3-ps duration. In addition, the calculations assume that the transition is homogeneously broadened, whereas strong experimental evidence exists that the $1s-2p^+$ transition is inhomogeneously broadened.¹² For these reasons, the value of the dephasing time $T_{12} = 18$ ps used in the two-level model should be viewed as an estimate of the inhomogeneous dephasing time only. The actual dephasing time can only be determined by comparison of the data with a full-model calculation that includes the exact pulse shape and details of the (inhomogeneously broadened) line shape. All essential features of the measurements, however, such as the node in Fig. 3(c), are reproduced by the calculations since they do not strongly depend on either the line shape or the exact pulse shape.

The time-dependent optical polarization radiates light with the transition frequency and the efficiency of the emission decreases when the polarization disappears. This is the so-called free-induction decay from which the

optical-dephasing time can be obtained.¹ Here, using the induced photoconductivity, we have measured the decay of the optical polarization which is the source of the free-induction decay emission, not the emission itself, to obtain the dephasing time. The method essentially frees us from the difficult problem of doing a time-resolved measurement of the (often) very weak far-infrared emission in the trailing wing of a pulse after it has propagated through the sample. By implication, we may be able to time resolve other optical coherent effects such as photon echoes, by combining photoconductivity measurements of the sample with the use of ultrashort pulses.

VI. CONCLUSIONS

We have used picosecond far-infrared pulse pairs from the FELIX to time resolve the free-induction decay of two Si-donor transitions in GaAs. Instead of detecting the light emission of the sample to measure the decay, we measure the decay of the optical polarization which is the source of the emission. We have shown that we can measure the polarization decay by measuring the ability of a second pulse to induce coherent changes in the population excited by a first pulse. We detect these population changes by measuring the photoconductivity of the sample.

ACKNOWLEDGMENTS

This work was performed as part of the research programme of the Stichting voor Fundamenteel Onderzoek der Materie (FOM) with financial support from the Nederlandse Organisatie voor Wetenschappelijk Onderzoek (NWO).

*FAX: +31 3402 31204. Electronic address: planken@zeus.rijnh.nl

¹A. E. Siegman, *Lasers* (University Science Books, Mill Valley, CA, 1986).

²Y. R. Shen, *The Principles of Non-Linear Optics* (Wiley, New York, 1984).

³G. R. Allan, A. Black, C. R. Pidgeon, E. Gornik, W. Seidenbusch, and P. Colter, *Phys. Rev. B* **31**, 3560 (1985).

⁴C. R. Pidgeon, A. Vass, G. R. Allan, W. Prettl, and L. Eaves, *Phys. Rev. Lett.* **50**, 1309 (1983).

⁵A. v. Klarenbosch, T. O. Klaassen, W. Th. Wenckebach, and C. T. Foxon, *J. Appl. Phys.* **67**, 6323 (1990).

⁶A. v. Klarenbosch, K. K. Geerincq, T. O. Klaassen, W. Th. Wenckebach, and C. T. Foxon, *Europhys. Lett.* **13**, 237

(1990).

⁷R. J. Bakker, C. A. J. van der Geer, D. A. Jaroszynsky, A. F. G. van der Meer, D. Oepts, and P. W. van Amersfoort, *Nucl. Instrum. Methods A* **331**, 79 (1993).

⁸R. Loudon, *The Quantum Theory of Light*, 2nd ed. (Clarendon, Oxford, 1983).

⁹P. C. M. Planken, I. Brener, M. C. Nuss, M. S. C. Luo, and S. L. Chuang, *Phys. Rev. B* **48**, 4903 (1993).

¹⁰P. C. Planken, I. Brener, M. C. Nuss, M. S. C. Luo, S. L. Chuang, and L. N. Pfeiffer, *Phys. Rev. B* **49**, 4668 (1994).

¹¹H. Friedrich and M. Chu, *Phys. Rev. A* **28**, 1423 (1983).

¹²C. J. Armistead, P. Knowles, S. P. Najda, and R. A. Stradling, *J. Phys. C* **17**, 6415 (1984).